

ENERGY LEVELS OF Re^{187}

R. G. ARNS[†] and M. L. WIEDENBECK

*Harrison M. Randall Laboratory of Physics,
The University of Michigan, Ann Arbor, Michigan*^{††}

Received 15 August 1960

Abstract: The gamma rays of Re^{187} following beta decay of the 24-hr W^{187} have been studied using prompt and delayed coincidence techniques. A total of 25 gamma rays was found. Relative intensities are given for the gamma transitions. The directional correlation of the 552-keV–134-keV cascade has been measured. A decay scheme is proposed on the basis of the coincidence measurements. Spins and parities of the principal levels are discussed.

1. Introduction

The decay of W^{187} ($\tau_{\frac{1}{2}} = 24$ hours) by beta emission to levels of Re^{187} has been studied by many authors¹⁻⁹. There has been general agreement regarding transitions connecting the levels at 686 keV, 206 keV and 134 keV. The 206-keV

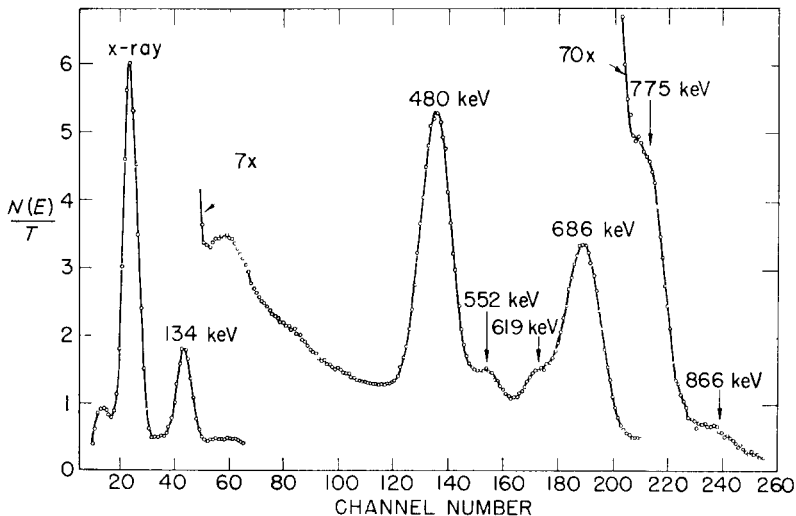


Fig. 1. Gamma-ray spectrum of W^{187} .

level is a metastable state with a half-life of $0.55 \mu\text{sec}$) A number of additional gamma rays have been known to exist²⁻⁵) but their position in a decay scheme has not been well established. The gamma ray spectrum of W^{187} , as shown in

[†] Present address: Department of Physics, The University of Buffalo, Buffalo, N. Y.

^{††} Work supported in part by the U. S. Atomic Energy Commission and the Michigan Memorial-Phoenix Project.

fig. 1, does not reflect this complexity. Hence it was felt that detailed coincidence measurements would be of value in establishing the existence and position of these weak gamma transitions.

Coulomb excitation of Re^{187} yields gamma rays of 134 keV, 167 keV and 301 keV¹⁰⁻¹⁵). Gamma-gamma coincidences have been observed following Coulomb excitation¹³). As a result of these measurements, a level has been proposed at 301 keV de-excited by a ground-state transition and a cascade through the 134-keV level. The 301-keV and 167-keV gamma rays have not previously been observed in the decay of W^{187} .

2. Experimental Procedure

The gamma coincidence measurements were made on samples of very pure tungsten foil which were irradiated at a flux of 2×10^{12} neutrons/cm²·sec for periods of 1 to 8 hours in the Ford Nuclear Reactor. A dilute solution of lithium tungstate was similarly irradiated to provide sources for the directional correlation measurements. The gamma ray spectrum of both forms of source material was followed for a one month period. The only activity observed in addition to the W^{187} was the long-lived electron-capture isotope, W^{181} . All data were taken early in the decay of each source in order to eliminate interference from W^{181} .

The prompt coincidence measurements employed a fast-slow coincidence circuit with a resolving time of 35 ns. A resolving time of 20 ns was used in the delayed coincidence measurements. Pulses coincident with a selected energy range were fed through a linear gate and recorded on a 256-channel analyzer.

The detectors in all cases consisted of 5.1 cm by 5.1 cm NaI(Tl) crystals mounted on R.C.A. 6342A phototubes. A Compton shield of 6.4 mm thick lead surrounded by 0.8 mm cadmium and 0.4 mm copper was placed between the detectors in the coincidence measurements.

Differential analyzers provided energy selection and lateral lead shielding was used to prevent counter-to-counter scattering in the directional correlation measurement. Data were taken in a double quadrant sequence at seven angles (i.e., every 15°) in each quadrant. The real coincidence rate was corrected for source decay and electronic drift. After making a least squares fit¹⁶), the expansion coefficients were normalized and corrected for finite resolution¹⁷).

3. Results

3.1. COINCIDENCE SPECTRA

Measurements were made of the spectra of gamma rays in prompt coincidence with 18 energy ranges. Delayed coincidence spectra involving the metastable state at 206 keV were observed in two additional measurements.

The spectra were corrected for random coincidences. The source to crystal distance in all cases was 2.5 cm. In order to eliminate coincidences with beta particles, the detectors were shielded frontally with 6.5 mm teflon in addition to the (1 mm) aluminium crystal case.

The results of all of the measurements are summarized in subsection 3.2. Only the most significant of the coincidence measurements will be displayed and discussed in detail here. These are listed below according to the energy range selected. The observed gamma ray energies are expected to be correct to within 1 %.

Coincidence with 125 keV to 145 keV

The spectrum of gamma rays coincident with the energy range from 125 keV to 145 keV is shown in fig. 2. The relative enhancement of the complex peak at 63 keV clearly illustrates the 72-keV-134-keV coincidence. The strong peak

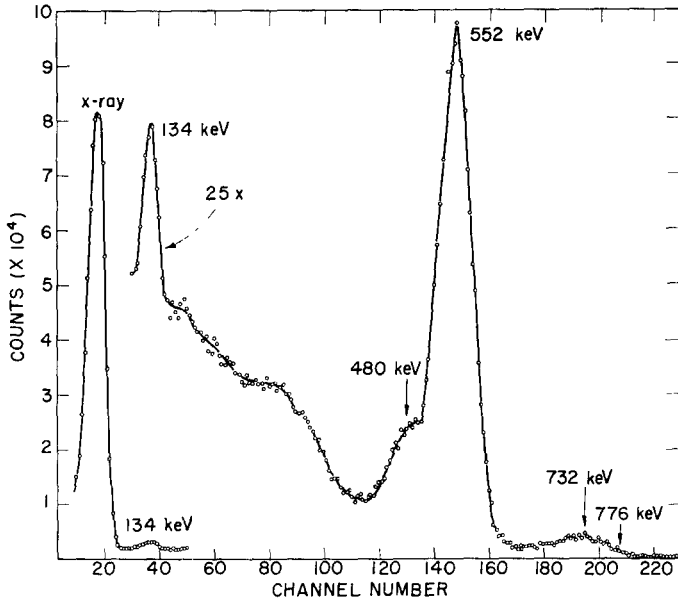


Fig 2 Spectrum of gamma rays coincident with the energy range from 125 keV to 145 keV.

at 552 keV is interpreted as a transition from the 686-keV level to the level at 134 keV. The peak at 480 keV is due to coincidences which pass through the metastable state at 206 keV. Considering the resolving time of the coincidence circuit and the lifetime of the 206 keV level, the intensity of this peak is consistent with the assumption that essentially all of the 480-keV transition decays through the metastable state. A new line is observed at 732 keV which is interpreted as a transition from a level at 866 keV to the 134-keV level. This peak may also contain a contribution from a weak line at 776 keV. The strong 775-

keV line observed in the singles spectrum is a ground-state transition. The 866-keV transition to the ground state appears in the singles spectrum but was not found in any of the coincidence spectra. The "continuum" from 175 keV to 400 keV is much larger than would be expected from the Compton distribution of higher energy gamma rays. This clearly indicates the presence of a number of unresolved lines.

Coincidence with 158 keV to 178 keV

Fig. 3 illustrates the gamma ray spectrum coincident with this energy range. A strong peak is observed at 301 keV. Fig. 6 will show this to be in coincidence with a line at 167 keV. New lines are noted at 440 keV and 485 keV. The bump

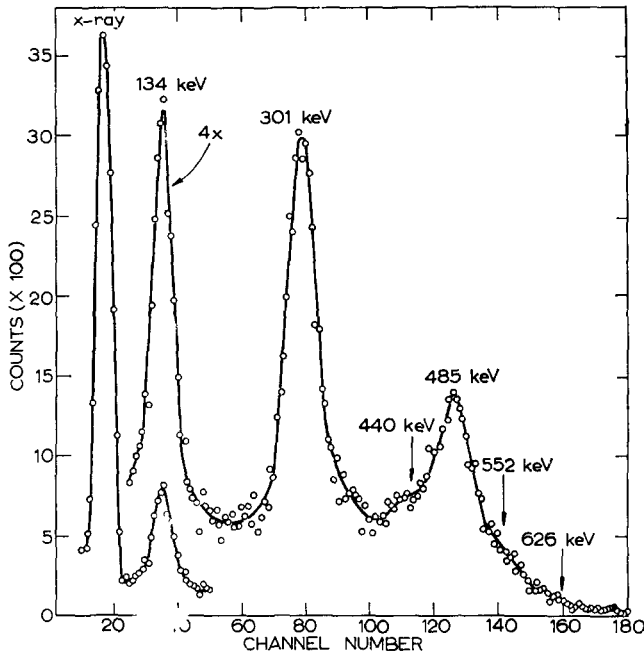


Fig. 3 Spectrum of gamma rays coincident with the energy range from 158 keV to 178 keV.

at about 364 keV is due to summing. The enhancement of the 63-keV peak and part of the 552-keV line are due to interference in the selector channel from the tail of the 134-keV line.

Coincidence with 180 keV to 225 keV

This coincidence spectrum is shown in fig. 4. The 485-keV line is quite strong. There is again a clear indication of a line at 440 keV. The 301-keV line is less intense since it is only coincident with the 167-keV transition. Lines of 552 keV, 626 keV, 686 keV and 760 keV are present, although quite weak. The 485-keV

line is clearly different from the 480 keV transition between the 686-keV and 206-keV levels. The presence of the 552-keV and 686-keV transitions indicates that a weak gamma ray of 180 keV (from the 866 keV level) feeds the 686-keV level. Again part of the 552-keV line appears to be the result of interference

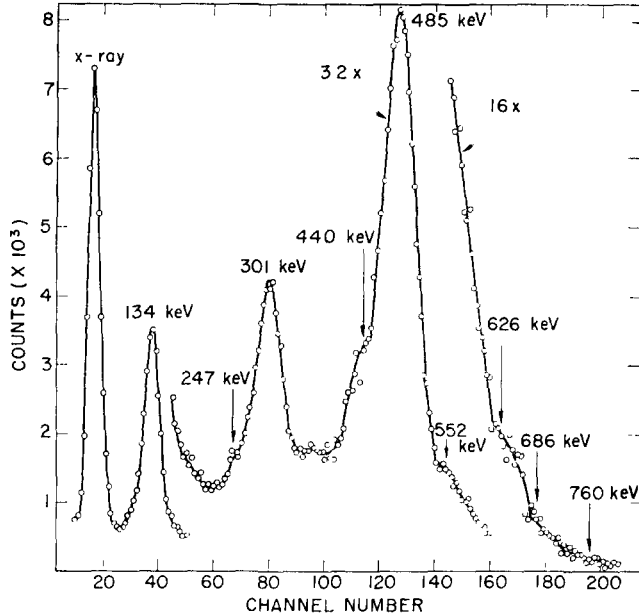


Fig 4 Spectrum of gamma rays coincident with the energy range from 180 keV to 225 keV

As will be seen below, the 485-keV line is apparently a ground state transition fed by a 201-keV transition from the level at 686 keV. The 760-keV line is probably also a ground state transition fed by a gamma ray in the energy range of this measurement. The 626-keV line is a transition from this new level to the first excited state. This was confirmed by other measurements.

Coincidence with 235 keV to 265 keV

This coincidence spectrum is shown in fig. 5. The principal line which is seen to be in coincidence with this energy region is at 619 keV. Additional weak lines are seen at 179 keV, 247 keV and 440 keV. The presence of the 134-keV line and its internal conversion X-ray is mostly due to interference from the Compton distribution of the 552-keV line in the energy selecting channel. The 247-keV line in this spectrum may similarly be explained as due to interference from the 619-keV line.

If a level is placed at 619 keV, which is principally de-excited by a ground state transition, then a 247-keV transition from the 866-keV level to the 619 keV level will give the observed strong coincidence. The 440-keV transition is

apparently also a ground state transition fed by a 179-keV transition from the 619-keV level.

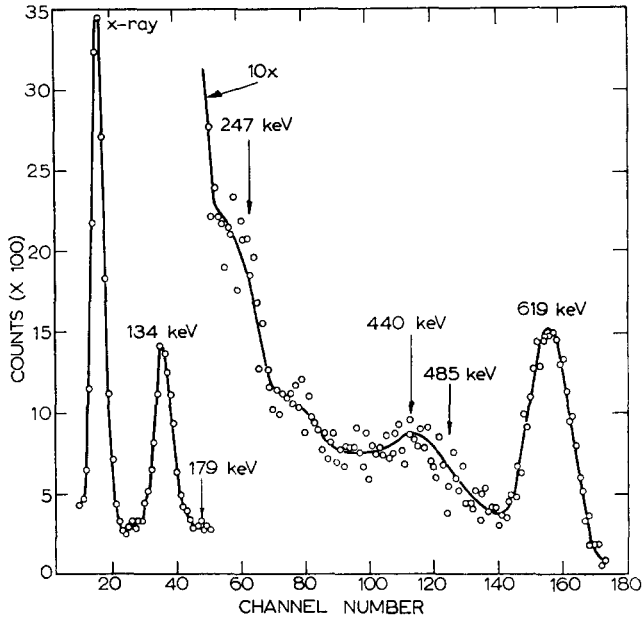


Fig 5 Spectrum of gamma rays coincident with the energy range from 235 keV to 265 keV

Coincidence with 285 keV to 315 keV

The spectrum of gamma rays coincident with this energy range is shown in curve A of fig. 6. Again, as in many of these curves, most of the 134-keV line

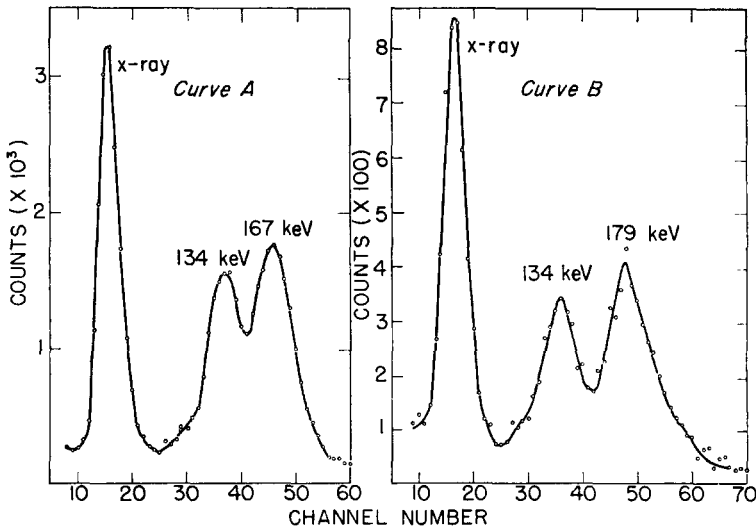


Fig 6 Curve A Spectrum of gamma rays coincident with the energy range from 285 keV to 315 keV Curve B Same for energy range from 425 keV to 455 keV

and its internal conversion X-ray is due to interference from the Compton distribution of the 552-keV line in the energy selecting channel. An additional strong line is seen at 167 keV. This is in coincidence with the 301-keV line as was seen in fig. 3.

Coincidence with 425 keV to 455 keV

This coincidence spectrum is shown in fig. 6, curve B. A strong coincidence is noted at 179 keV. The two parts of fig. 6 illustrate that the 167-keV and 179-keV lines are clearly distinct.

Coincidence with 455 keV to 505 keV

The spectrum of gamma rays in prompt coincidence with this energy region is shown in curve A of fig. 7. Again the 134-keV line and its X-ray appear as a result

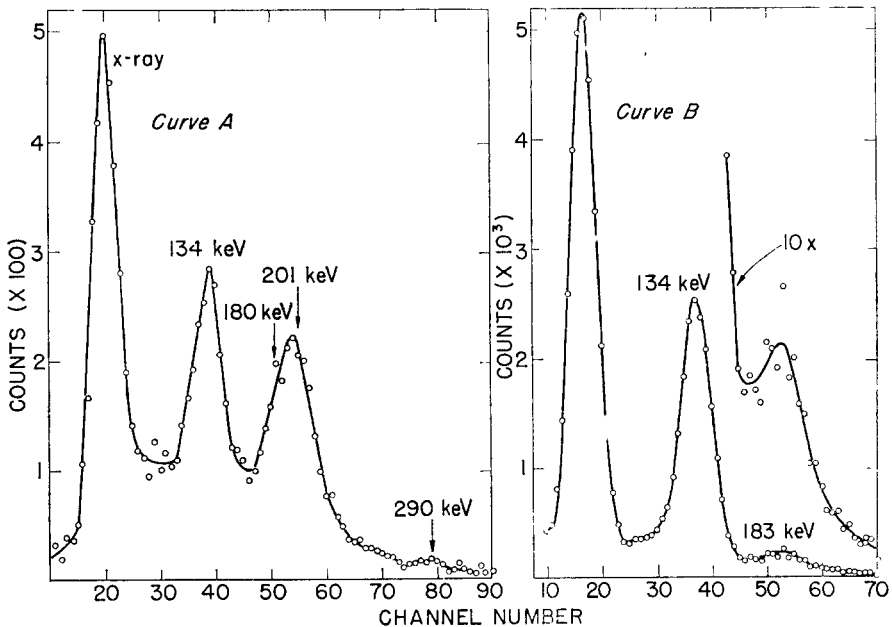


Fig. 7. Curve A. Spectrum of gamma rays coincident with the energy range from 455 keV to 505 keV. Curve B. Same for energy range from 535 keV to 585 keV.

of the interference. A complex line centered at ≈ 198 keV is found. The major part of this coincidence is due to the 201-keV transition to the 485-keV level. The remainder results due to the tail of the 440-keV line in the selector channel which permits the 179-keV line to appear. A weak line is seen at about 290 keV. This may indicate a weak transition of this energy from the 775-keV level to the 485-keV level.

Coincidence with 535 keV to 585 keV

This coincidence spectrum is shown in fig. 7, curve B. The principal transition in coincidence with this energy range is the 134-keV transition from the first excited state to the ground state. This spectrum provides an excellent means of determining the K-conversion coefficient of the 134-keV transition as will be seen below. The additional weak line at about 180 keV is partly due to the transition from the 866-keV level to the 686-keV level and partly the result of interference from the 626-keV–185-keV coincidence (cf. below).

Coincidence with 610 keV to 650 keV

This coincidence spectrum is shown in fig. 8. The 134-keV transition is seen to be in coincidence with a gamma ray in this energy range. In addition, coincidences are observed with gamma rays at 185 keV and 247 keV. The 247-keV gamma ray is interpreted as a transition from the 866-keV level to the 619-keV level and is in coincidence with the ground state transition from the latter level. A 626-keV gamma ray from a level at 760 keV to the first excited state gives rise to the coincidence with the 134-keV transition. The 185-keV gamma ray is probably a transition from a level at 945 keV to the 760-keV level.

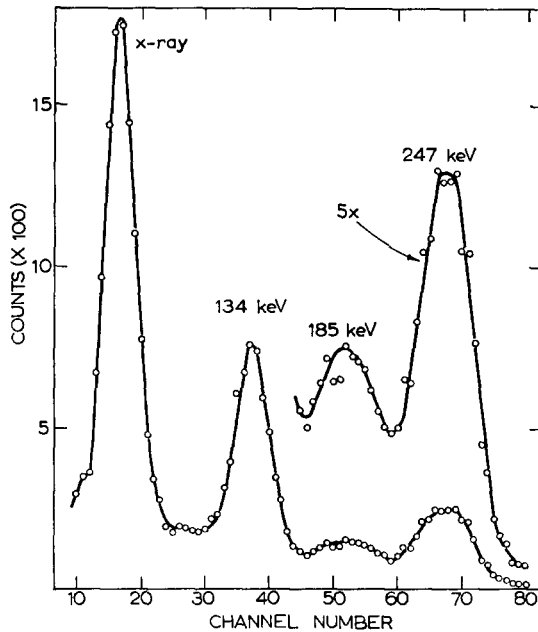


Fig 8 Spectrum of gamma rays coincident with the energy range from 610 keV to 650 keV

Delayed coincidence with the 134-keV gamma ray

Fig. 9, part A shows the coincidence spectrum which is observed by accepting the 134-keV gamma ray in the selector channel and delaying the pulses which

are to be displayed on the multichannel analyzer by 220 ns. In this way prompt coincidences are minimized and the gamma rays which pass through the

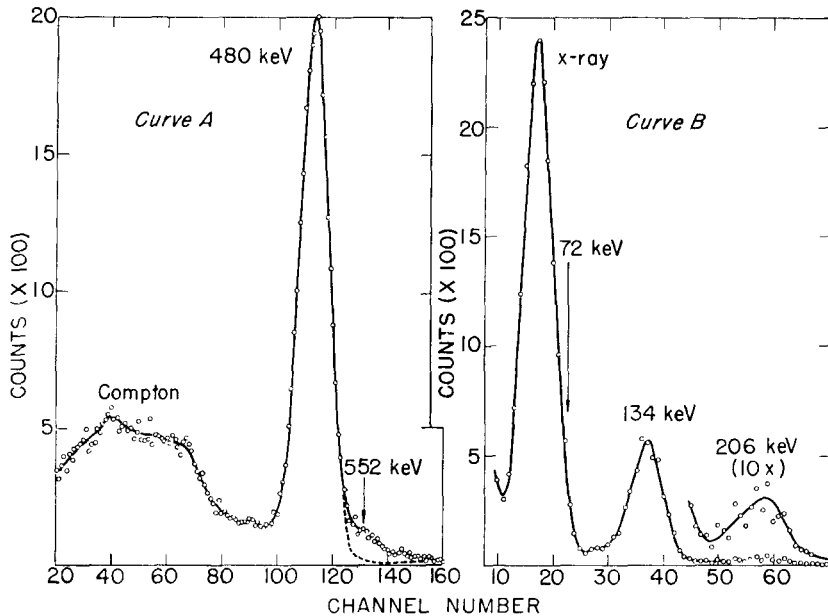


Fig 9 Curve A Spectrum of delayed coincidences with the 134-keV gamma ray Curve B Spectrum of delayed coincidences with the 480-keV gamma ray

metastable state at 206 keV may be observed. The 480-keV transition from the 686 keV level to the metastable state is the only delayed coincidence which appears. A small peak is present at 552 keV due to prompt coincidences.

Delayed coincidences with the 480 keV line

If pulses from the detector in the range selector channel are delayed by 220 ns and if this channel is set to accept the 480-keV peak, then the multichannel analyzer will display only gamma rays from the decay of the metastable state. This is shown in part B of fig. 9. Some of the X-ray and 134-keV peaks will result from prompt coincidences due to interference from the 552-keV Compton distribution in the selecting channel. After this correction is made, this curve serves as a means of determining the unconverted relative intensity of the 206-keV crossover transition from the metastable state.

3.2 SUMMARY OF THE COINCIDENCE MEASUREMENTS

In addition to the coincidence spectra discussed in section 3.1, a number of other measurements were made. These are summarized, along with the data described above, in table I.

TABLE 1
Summary of the coincidence measurements

Energy range (keV)	Observed coincident gamma ray energies (keV)																						
	x-ray + 72	134	167	179 +	180	185	201	206	247	290	301	440	480	485	552	619	626	686	732	760	775 +	866	
65-90	s	s											m		s		vW	x	m		vW	x	
125-145	s	m			vW								m		s		vW	x	m		vW		
158-178	s	s	x	x	x			x	vW		s	m		s	w		vW	vW			vW		
180-240	s	s	x					x	w		m	m		s	w		w	vW			vW		
180-225	s	s	x					x	w		m	m		s	w		m	w			w		
225-275	s	s	x	vW				x	vW		x	m		m		s							
235-265	s	s	x	vW				x	vW		x	m		w		s							vW
280-340	s	s	s					x	vW		x	x		vW		vW							
285-315	s	s	s					x	vW		x	x		vW									
360-420	m	m		m				x	vW		x	x											
425-455	m	m		s				x	vW		x	x											
455-505	m	m		w						w	x	x											
474-491	m	m		vW	vW					vW	x	x											
535-585	s	s		vW	w			x			x												
610-650	m	m			m			x	m		x												
675-697	vW	vW		vW				x			x												
740-800	vW	vW			vW			x															
840-880	x	x																					
Delayed 134													s		w								
Delayed 480	s	s						w															

s = strong conc., m = medium conc., w = weak conc., v = very weak conc., x = not in coincidence. A blank square does not indicate the absence of a coincidence. Often neighbouring strong peaks may overwhelm a weak transition or a number of close peaks may be unresolved.

3.3 INTERNAL CONVERSION MEASUREMENTS

A number of electron lines from W^{187} were observed by Cork *et al.*³⁾ in photographic magnetic spectrometers. The W^{187} sources were produced by neutron bombardment of isotopically-enriched (97.5 %) W^{186} . Their data have been reinterpreted and the results are summarized in table 2. Many of the weak

TABLE 2
Energies of electron conversion lines as observed by Cork *et al.*³⁾

Electron energy (keV)	Interpretation	Energy sum (keV)	Electron energy (keV)	Interpretation	Energy sum (keV)
34.5	K	106.2	134.5	K	206.2
41.9	K	113.6	167.5	K	239.2
46.6	Auger ($\alpha_1 - L_1$)		174.6	K	246.1
48.7	Auger ($\alpha_1 - L_3$)		194.2	L_2	206.2
50.3	Auger ($\alpha_2 - L_3$)		203.3	M	206.2
59.5	L_1	72.0 ^{a)}	229 ^{a)}	K	301
61.5	L_3	72.0	395 ^{a)}	K	467
62.5	K	134.2 ^{b)}	408	K	479.5 ^{b)}
69.3	M	72.0	468	L	479.5
71.7	N	72.0	480	K	552
94.2	L_2	106.2	547	K	618.9 ^{b)}
101.6	L_2	113.6	554 ^{a)}	K	626
110.3 ^{a)}	K	182.0	607	L	619
121.7	L_1	134.2	614	K	686.1 ^{b)}
122.2	L_2	134.2	674	L	686.1
123.7	L_3	134.2	703	K	775
131.4	M	134.2	763	L	775
133.6	N	134.2	794	K	866

a) Weak and uncertain lines

b) Crystal spectrometer values of Muller *et al.*²⁾

lines observed in the coincidence measurements are below the limit of observation of the internal conversion experiment. Similarly three of the lines found in internal conversion (106.2 keV, 113.6 keV and 467 keV) were not seen in the coincidence measurements.

Vergnes^{8,9)} has summarized the measurements of K-shell internal conversion coefficients for the strong transitions in Re^{187} . These data are shown in table 3.

The spectrum of gamma rays coincident with the 552-keV transition in the present experiment provided an accurate determination of α_K for the 134 keV transition. Using the X-ray and 134-keV photopeak intensities, and correcting for absorption, crystal efficiency and X-ray fluorescence yield, a value of $\alpha_K = 1.75 \pm 0.14$ was determined. As is seen in table 3, this is consistent with the assumption that the 134 keV transition is predominantly M1 with a small E2 admixture.

TABLE 3
K-shell internal conversion coefficients for strong transitions in Re¹⁸⁷

E_γ (keV)	α_K (exp)	α_K (theor.)				Multipolarity
		E1	E2	M1	M2	
72	1.4 ± 0.2	0.61	1.06	9.6	81	E1 + M2 (or E2 + M1)
134	1.5 ± 0.4	0.15	0.47	1.9	11.4	M1 + E2 (or E1 + M2)
	$2.12 \pm 0.32^a)$					
	$1.75 \pm 0.14^b)$					
480	0.0195	0.0067	0.018	0.056	0.16	E2
552	0.029	0.005	0.013	0.04	0.11	E1 + M2 or E2 + M1
619	0.06	0.004	0.01	0.03	0.08	E1, E2 or M1
686	0.0069	0.0032	0.0082	0.023	0.06	E1
775	0.047	0.0025	0.0065	0.017	0.042	M2

Unless otherwise noted, the experimental coefficients are due to Vergnes^{8,9)}. The theoretical values were obtained from the tables of Sliv and Band¹⁸⁾.

a) McGowan and Stelson¹⁴⁾. b) Present measurement.

It is not possible to assign a unique multipolarity to the 72-keV or 134-keV transitions on the basis of the K-shell conversion alone. The experimental L-shell internal conversion coefficients measured by Vergnes^{8,9)} are compared to corresponding theoretical values in table 4. This comparison shows clearly that the 72 keV transition is predominantly E1 with a small M2 admixture ($M2 \leq 1.5\%$).

TABLE 4
L-shell internal conversion data for the 72-keV and 134-keV transitions in Re¹⁸⁷

E (keV)	Experimental coefficient	Ref	Theoretical coefficient			
			E1	E2	M1	M2
72	$\alpha_{L_1 + L_2} =$ 0.23 ± 0.13	8,9)	0.083	4.5	1.396	28.6
134	$\alpha_L = 0.3 \pm 0.1$ $K/L = 4.6 \pm 0.5$	8,9)	0.026	0.66	0.31	3.4
		10)	5.8	0.71	6.1	3.3

Although the L-shell conversion data for the 134 keV transition supports an M1(+E2) assignment for the 134 keV transition, it does not rule out an E1 + M2 mixture. However, the Coulomb excitation of the 134-keV level rules out the latter assignment and it can be concluded from the internal conversion data that the 134-keV transition is mostly M1 with an E2 content of $< 25\%$.

3.4 GAMMA-RAY RELATIVE INTENSITIES

The relative intensities of the observed gamma rays were determined from the singles and coincidence spectra. The results are summarized in table 5. The intensities have been corrected for efficiency and absorption due to the shields covering the front of the crystals. The relative intensities of the stronger transitions have been determined by a least-squares fitting of the individual gamma-ray distributions to the observed singles spectrum. Details of this

TABLE 5
Relative intensities of the gamma rays from W^{187}

E_γ (keV)	Relative intensity ^{a)}	Estimated uncertainty (%)	Transition intensity (%)
72	65.7	± 20	21.5 ^{b)}
134	47.2	± 10	30.4 ^{b)}
167	4.8	± 20	1.1
179	2.6	± 40	0.61
180	0.05	± 50	0.012
185	0.05	± 50	0.012
201	4.1	± 40	0.96
206	2.2	± 50	1.9 ^{c)}
247	0.19	± 30	0.044
290	0.50	± 40	0.12
301	4.8	± 20	1.12
440	2.6	± 40	0.61
480	100		23.4
485	4.6	± 40	1.2
552	28.7	± 10	6.7
619	38.9	± 10	9.1
626	0.85	± 50	0.2
686	134	± 5	31.4
732	2.8	± 20	0.65
760	0.15	± 50	0.035
775	20.3	± 10	4.75
776	1.1	± 40	0.25
866	3.5	± 10	0.82

The relative intensities of the unconverted gamma rays are compared to the 480-keV gamma ray. An estimate of the uncertainty in the relative intensity is given in the third column. The transition intensities have been corrected for internal conversion wherever possible.

a) Unconverted gamma ray intensity.

b) Internal conversion from tables 3 and 4.

c) Theoretical M2 internal conversion.

method will be published elsewhere¹⁹⁾. In this manner accurate relative intensity values were obtained for the 480 keV, 552 keV, 619 keV, 686 keV, 775 keV and 866 keV gamma rays. All of the other intensities were obtained by comparing photopeak areas in the singles and coincidence spectra.

3.5 DIRECTIONAL CORRELATION MEASUREMENT OF THE 552-keV-134-keV CASCADE

In measuring the directional correlation of this cascade, each of the differential analyzers was allowed to accept a narrow range of the full-energy peak of one of the gamma rays. The resultant expansion coefficients, after correction for finite angular resolution, were found to be $A_2 = 0.316 \pm 0.018$ and $A_4 = -0.086 \pm 0.027$. Some interference was present due to the tail of the 480-keV gamma ray in the channel accepting the 552-keV photopeak. The contribution from this source was found to be $3 \pm 2\%$ of the total coincidence rate and can be expected to be isotropic due to the intermediate metastable state. As is clearly shown in fig. 2, interference from higher energy gamma rays in the 552-keV channel is also very small. No correction was made for these effects.

The ground state spin of Re^{187} has been measured²⁰⁾ to be $\frac{5}{2}$. Re^{187} has 75 protons. The ground state is logically characterized in terms of the Nilsson model^{21, 22)} as $\frac{5}{2}^+$. This corresponds to an equilibrium deformation parameter of $\delta = 0.19$. The Nilsson diagram predicts that the next intrinsic excitation will have a spin and parity of $\frac{3}{2}^-$. This appears to correspond to the metastable state at 206 keV. The first excited state at 134 keV does not fit the Nilsson diagram as an intrinsic level. It is most easily characterized as the first rotational excitation of the ground-state configuration. If this is indeed the case, this level will have a spin and parity of $\frac{7}{2}^+$. This is consistent with the Coulomb excitation^{10, 15)} of this level and with the internal conversion data. Thus it seems safe to assume that the 134-keV gamma ray is a $\frac{7}{2}$ (M1 + E2) $\frac{5}{2}$ transition with a quadrupole content of $Q \leq 0.25$ (from internal conversion data). If the above spin and parity assumptions are indeed correct, then the pattern of transitions from the 686-keV level to the ground state and first two excited states is only consistent with spin assignments of $\frac{5}{2}$, $\frac{7}{2}$, or $\frac{9}{2}$ to the 686-keV level. Of these possibilities only $\frac{7}{2}$ will fit the observed directional correlation expansion coefficients. The negative A_4 coefficient is inconsistent with the $\frac{5}{2}$ or $\frac{9}{2}$ assignments. If the quadrupole content of the second transition is assumed to be $Q_2 \leq 0.25$, then the $\frac{7}{2}(D_1, Q_1)\frac{7}{2}(D_2, Q_2)\frac{5}{2}$ sequence will fit the measured coefficients over a considerable range of Q_1 . This is shown in fig. 10²³⁾.

As is seen from the graphical analysis, the large A_2 coefficient requires a large partial coefficient for each transition ($A_2 = A_2^{(1)} A_2^{(2)}$). Measurements of the angular distribution of the 134-keV gamma ray following Coulomb excitation^{14, 15)} have been found to be isotropic. As can be seen from the $\frac{7}{2}(D, Q)\frac{5}{2}$ curve in fig. 10, this requires a quadrupole content of about 3% in the 134-keV transition. This is clearly in disagreement with the present directional correlation expansion coefficients. Mössbauer and Wiedemann²⁴⁾ have measured the half-life of the 134-keV level to be $\tau_{\frac{7}{2}} = (1.04 \pm 0.14) \times 10^{-11}$ sec. The sources used in the Coulomb-excitation experiment were metallic rhenium (which has a hexagonal crystal structure). It is possible that the angular distribution was perturbed in the Coulomb excitation measurement.

If the parity of the 686-keV level is even, this would then contradict the measured internal conversion of the ground state transition (E1, see table 3). A $\frac{7}{2}$ - assignment for this level will make the 686-keV transition an E1, the 480-keV transition an E2 + M1 mixture, and the 552-keV transition an E1 + M2 mixture, in keeping with the internal conversion measurements. The mixing ratios implied for the 480-keV transition and the 552-keV transition are rather large. Vergnes⁸⁾ has pointed out that the 686-keV E1 gamma ray is highly hindered. Re¹⁸⁷ is in the transition region between the highly-deformed rotational nuclei and the nuclei with small equilibrium deformation. Here

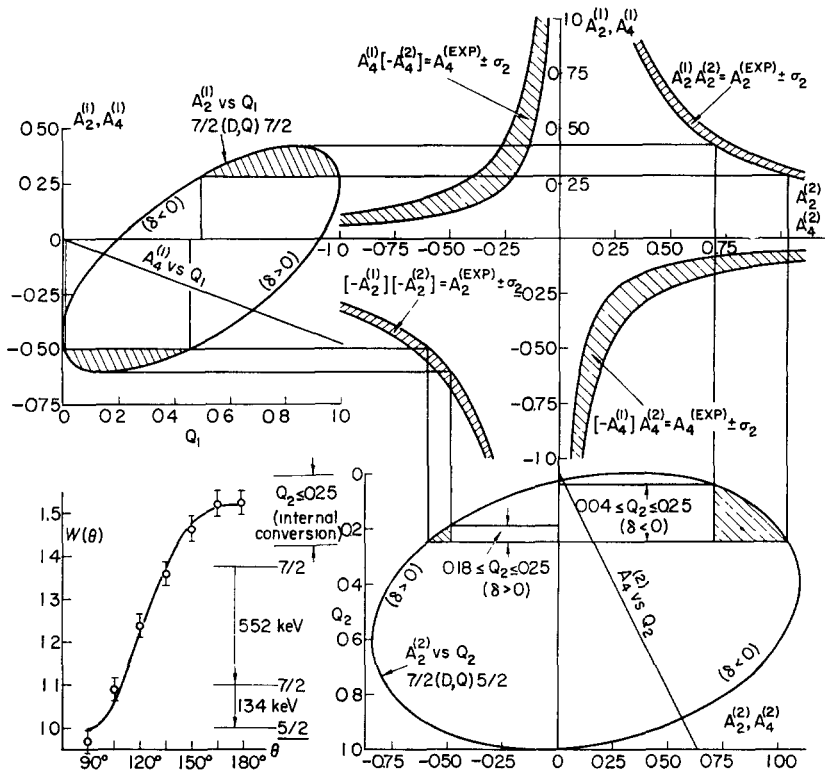


Fig 10 Graphical analysis of the 552-keV-134-keV directional correlation data in terms of a $\frac{7}{2}(D, Q)\frac{7}{2}(D, Q)\frac{7}{2}$ sequence. Internal conversion data have been used to limit the allowed range of quadrupole mixture in the second transition. The insert in the lower left corner shows the corrected experimental points and the resultant least-squares curve for the correlation function $W(\theta)$

intrinsic excitations may occur involving a change of nuclear deformation²²⁾. If the 686-keV level does involve an excitation of this nature, the observed mixing ratios would be entirely reasonable.

It does not seem possible that the observed A_4 coefficient is in error. Sufficient precautions were taken to avoid counter-to-counter scattering. A second measurement, made under different conditions, gave similar results although

attenuation was present due to source environment. The $\frac{7}{2}$ assignment to the 686-keV level is based on the presence of the A_4 coefficient. The A_2 coefficient alone would be consistent with sequences of the form $\frac{3}{2}(D, Q)\frac{1}{2}(D, Q)\frac{5}{2}$ or $\frac{5}{2}(D, Q)\frac{1}{2}(D, Q)\frac{5}{2}$.

Although directional correlation measurements on other cascades in Re^{187} would be desirable, intensity considerations or interference make these unprofitable. Previous measurements on the 72-keV–134-keV cascade^{6,7)} suffer from the isotropic contribution of the unresolved X-ray in the channel accepting the 72-keV line. Due to these difficulties, no attempt was made to repeat the measurement.

4. Discussion

In subsections 3.1 and 3.2 the observed coincidence spectra were summarized and some arguments for the level structure of Re^{187} were given. The proposed decay scheme is shown in fig. 11. The levels and the transitions connecting them

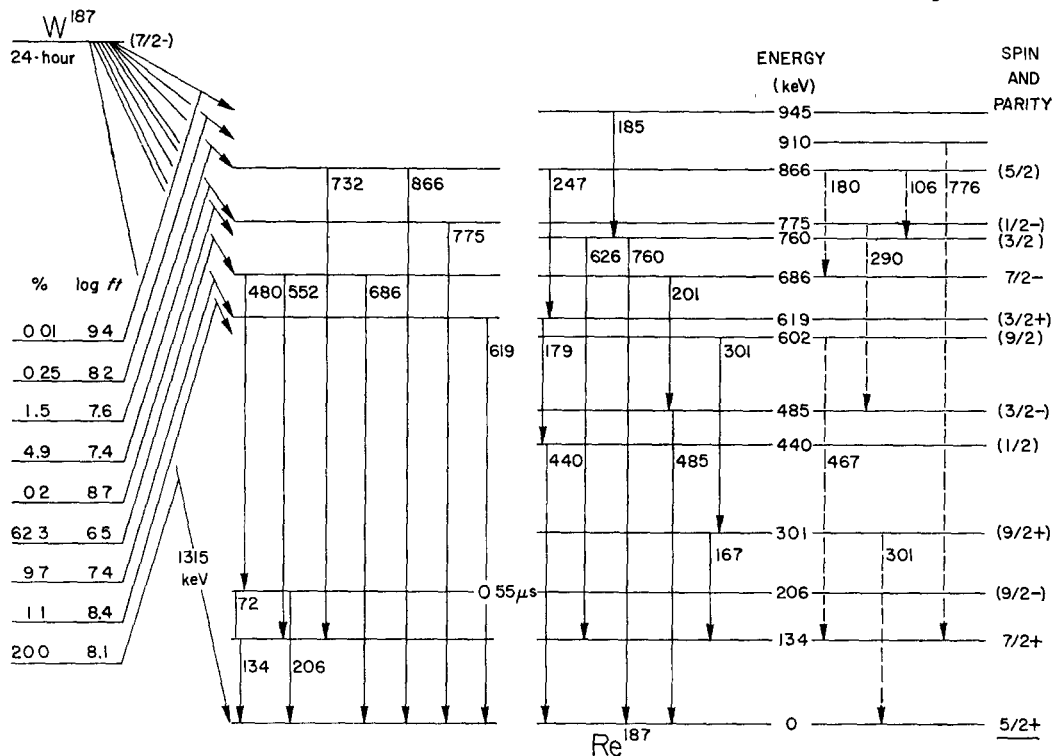


Fig 11 Decay scheme of W^{187} . The level structure has been divided into three sections dependent upon the strength of the evidence for the proposed transitions and levels. The position and existence of transitions shown in the left-hand portion of the decay scheme are known with certainty. The position of gamma rays shown in the centre section of the decay scheme is probable. The gamma rays shown in the right-hand section of the decay scheme are very weak and the position proposed is not certain. The $\log ft$ values have been computed assuming a 20% ground-state component^{3,5)} and using the gamma transition intensities given in table 5.

have been divided into three groups dependent upon the strength of evidence for their existence and position. In order to clarify the arguments leading to this level structure and simplify the interpretation, each level will be discussed separately.

The 134-keV level

There is ample evidence that the first excited state of Re^{187} occurs at 134 keV. The 134 keV gamma ray has been observed in Coulomb excitation¹⁰⁻¹⁵) and resonance fluorescence²⁴) experiments, and following the beta decay of $\text{W}^{187\text{I}-9}$). The latter measurements have shown that this level is fed by gamma rays of 72 keV and 552 keV from the 206-keV and 686-keV levels respectively. The present coincidence measurements have shown the existence of weak feeding by gamma rays of 626 keV, 732 keV, 167 keV, and perhaps 776 keV. The possibility of additional beta feeding from W^{187} was investigated by Vergnes^{8,9}). He placed an upper limit of 5% on the portion of the total number of beta transitions which feed this level. This is in accord with the present measurements.

The probable spin and parity assignment for this level ($\frac{7}{2}^+$) has been discussed in detail in subsection 3.5.

The 206-keV level

The metastable state at 206 keV is fed by a 480-keV gamma transition from the 686-keV level. It is de-excited mainly by a 72-keV E1 transition to the first-excited state (cf. subsection 3.3). The ground state transition from the 206-keV level is quite weak. Again, as for the 134-keV level, there does not appear to be significant beta feeding of this level.

In accord with the E1 multipolarity of the 72-keV transition to the $\frac{7}{2}^+$ first-excited state, possible spin and parity assignments for the 206-keV level are $\frac{9}{2}^-$, $\frac{7}{2}^-$, or $\frac{5}{2}^-$. Thus the 206-keV transition can be M2 or E1. The relative weakness of this transition favors an M2 multipolarity and hence the $\frac{9}{2}^-$ assignment for the 206-keV level. The Nilsson model predicts a $\frac{9}{2}^-$ orbit in this region^{21,22}). This has been observed at 496 keV in $\text{Re}^{183\text{I}25}$).

The half-life of the 206-keV state is¹⁾ 0.55 μsec . This lifetime clearly shows that the 72-keV E1 transition is highly hindered. Presumably this is a K-forbidden transition in which case the observed retardation is as predicted.

The 301-keV level

Gamma rays of 134 keV, 167 keV and 301 keV have been observed in Coulomb excitation of $\text{Re}^{187\text{I}10-15}$). As a result of these experiments, a level at 301 keV has been proposed which is deexcited by a ground-state transition and a cascade through the 134-keV level. This level has been interpreted as the third member ($\frac{9}{2}^+$) of the ground-state rotational band.

In the present experiment gamma rays of 167 keV and 301 keV have been observed and have been shown to be in coincidence (cf. figs. 3 and 6A). Although the possibility that the 301-keV–167-keV cascade reaches the ground state directly cannot be ruled out on the basis of the coincidence measurements, it is probable that this cascade feeds the first-excited state. Aside from the 301-keV, 167-keV, and probably the 134-keV gamma rays, no other coincidences were observed in this sequence. If the 167-keV gamma ray is a transition from the 301-keV level to the first excited state, then the observed 301-keV gamma ray must feed the 301-keV level. It is possible that the 167-keV and 301-keV gamma rays observed in this experiment differ from those following Coulomb excitation. However, if the same levels are involved, one is forced to conclude that the crossover transition from the 301-level is weaker than had been supposed.

The 440-keV level

A new level is proposed at 440 keV which is fed by a 179-keV gamma ray from the 619-keV level and de-excited by a ground-state transition. Evidence for this cascade appears in figs. 4 and 6B. Fig. 5 supports the conclusion that this cascade deexcites the 619 keV level. Decay of the 440-keV level to the ground state but not to the 134-keV, 206-keV, or 301-keV levels favors a low spin, perhaps $\frac{1}{2}$, for this level.

The 485-keV level

Figs. 3 and 4 show the existence of a line of about 485 keV which is different from the 480-keV transition (between the 686-keV and 206-keV levels). Fig. 7A shows the origin of this coincidence as a 201-keV–485-keV cascade, which apparently de-excites the 686-keV level. Fig. 7A also indicated a weak 290-keV–485-keV coincidence. The 290-keV gamma ray is probably a transition between the 775-keV and 485-keV levels. As in the case of the 440-keV level, the direct decay to the ground state favors a low spin for the 485-keV level.

The 602-keV level

The 602-keV level has been postulated in order to explain the observed 301-keV–167-keV coincidence. The arguments regarding the position of this cascade have been given above in the discussion of the 301-keV level. A weak 467-keV gamma ray was observed in the internal-conversion measurements (cf. table 2) which may correspond to a transition between the 602-keV level and the first-excited state. Since no gamma rays are observed feeding the 602-keV level, it is presumably fed by a separate beta transition. The pattern of transitions from this level favors a spin of $\frac{3}{2}$.

The 619-keV level

The 619-keV level is de-excited by a strong ground-state transition and by a weak cascade through the 440-keV level. It is fed mainly by a beta transition

from W^{187} . Additional weak feeding by a 247-keV gamma ray from the 866-keV level is indicated in the coincidence spectra (cf. figs. 5 and 8).

A low spin is favored by the direct ground-state decay from this level. If the W^{187} ground state is characterized as $\frac{7}{2}-$ (cf. below), a $\frac{3}{2}+$ assignment to the 619-keV level would require a first-forbidden beta decay to this level in accord with observed $\log ft = 7.4$.

The 686-keV level

The 686-keV level is fed mainly by a strong beta transition from W^{187} and de-excited by strong gamma rays of 480 keV, 552 keV and 686 keV. An additional weak 201-keV gamma ray from this level has been discussed above in regard to the 485-keV level. Evidence for a very weak 180-keV gamma ray feeding the 686-keV level appears in the coincidence measurements (cf. table 1).

The assignment of a spin and parity of $\frac{7}{2}-$ to the 686-keV level has been discussed in detail in subsection 3.5. In accord with the Nilsson model, possible spin and parity assignments for the W^{187} ground state are $\frac{1}{2}-$, $\frac{3}{2}-$, or $\frac{7}{2}-$. The observed $\log ft$ (6.5) of the beta transition to the 686-keV level ($\frac{7}{2}-$) rules out $\frac{1}{2}-$ and $\frac{3}{2}-$. A $\frac{7}{2}-$ assignment for the W^{187} ground state would characterize this beta transition as allowed hindered. Beta decay to the ground state and 134-keV and 206-keV levels also appears to be hindered.

The 760-keV level

The presence of a coincidence between the 134-keV gamma ray and a gamma ray in the region 610 keV to 650 keV was shown in fig. 8. It seems reasonable that this coincidence arises from the 626-keV gamma ray observed by Cork *et al.*³⁾ (cf. table 2). This then necessitates the placing of a level at 760-keV. Both the 626-keV and 760-keV gamma rays appear in coincidence with a gamma ray in the region 180 keV to 225 keV (cf. fig. 4). Fig. 8 shows the energy of this transition to be 185 keV. The 760-keV level is partly fed by a beta transition. A weak transition 106 keV, observed only in internal conversion (cf. table 2), has been shown in the decay scheme feeding the 760-keV level.

The pattern of transitions from this level favor a spin assignment of $\frac{3}{2}$.

The 775-keV level

The observed M2 multipolarity of the 775-keV ground-state transition (cf. table 3) favors a spin and parity of $\frac{1}{2}-$ for this level. The $\log ft = 7.4$ of the beta transition feeding this level is then difficult to explain.

The 866-keV level

Evidence for the placing of a level at 866-keV includes the presence of a ground-state transition and 732-keV and 247-keV transitions to the 134-keV and 619-keV levels respectively. An additional weak transition of 180-keV to

the 686-keV level has also been proposed. This level is apparently fed by a separate beta transition from W^{187} . A spin assignment of $\frac{5}{2}$ or $\frac{3}{2}$ seems to be favored by the observed gamma de-excitation.

The 910-keV level

The weak 776-keV–134-keV coincidence suggests the placing of a beta-fed level at 910 keV.

The 945-keV level

The 185-keV transition to the 760-keV level de-excites a beta-fed level at 945 keV.

References

- 1) McGowan, DeBenedetti and Francis, Phys. Rev. **75** (1949) 1761
- 2) Muller, Hoyt, Klein and DuMond, Phys. Rev. **88** (1952) 775
- 3) Cork, Brice, Nester, LeBlanc and Martin, Phys. Rev. **89** (1953) 1291
- 4) A W Sunyar, Phys Rev **90** (1953) 387A
- 5) Dubey, Mandeville, Mukerji and Potnis, Phys Rev **106** (1957) 785
- 6) H J Behrend and H Neuert, Z Naturforsch., **13a** (1958) 208
- 7) M. V Klimentovskaya and P I Shavrin, JETP **36** (1959) 1360
- 8) M Vergnes, J. Phys. Rad. **19** (1958) 947
- 9) M Vergnes, Ann de Phys. **5** (1960) 11
- 10) E M. Bernstein and H. W. Lewis, Phys Rev **105** (1957) 1524
- 11) G Goldring and G. Paulissen, Phys Rev. **103** (1955) 1314
- 12) Davis, Divatia, Lind and Moffat, Phys Rev **103** (1956) 1801
- 13) Wolicki, Fagg and Geer, Phys Rev. **105** (1957) 238
- 14) F K McGowan and P H. Stelson, Phys Rev. **109** (1958) 901
- 15) de Boer, Martin and Marmier, Helv Phys Acta **32** (1959) 377
- 16) M. E Rose, Phys Rev. **91** (1953) 610
- 17) Arns, Sund and Wiedenbeck, Univ. of Mich. Res Inst Report 2375-4-T, February 1959
- 18) L. A Shiv and I M Bond, Leningrad Phys. Techn Inst Rep 1956 (translations Report 57 ICC KI, Phys Dep. University of Illinois, Urbana, Illinois)
- 19) J. Trombka and M L Wiedenbeck, Univ of Mich. Res. Inst. Report 2863-2-P, September 1960
- 20) S L. Segel and R G Barnes, Phys. Rev **107** (1957) 638
- 21) S. G Nilsson, Mat. Fys Medd Dans Vid Selsk **29**, No 16 (1955)
- 22) B R Mottelson and S. G. Nilsson, Mat. Fys. Skr. Dans Vid Selsk **1**, No. 8 (1959)
- 23) R G Arns and M L. Wiedenbeck, Phys Rev **111** (1958) 1631
- 24) R L Mossbauer and W H Wiedemann, Zeit. f Phys. **159** (1960) 33
- 25) J O Newton and V S Shirley, Bull Am Phys Soc. **2** (1957) 395